ENTROPY PRODUCTION AND THE G-SCHEME

Mauro Valorani*, Samuel Paolucci**

*Mechanical and Aerospace Engineering, Sapienza University of Rome, Rome, Italy
**Aerospace and Mechanical Engineering, University of Notre Dame, Notre Dame, IN, USA

ABSTRACT

Spatially homogeneous batch reactor systems are characterized by the simultaneous presence of a wide range of time scales. When the dynamics of such reactive systems develop very-slow and very-fast time scales separated by a range of active time scales, with large gaps in the fast/active and slow/active time scales, then it is possible to achieve multi-scale adaptive model reduction along-with the integration of the governing ordinary differential equations using the G-Scheme framework. The G-Scheme assumes that the dynamics is decomposed into active, slow, fast, and when applicable, invariant subspaces. We computed the contribution to entropy production by the four subspaces, with reference to a constant volume, adiabatic reactor. The numerical experiments indicate that the contributions of the fast and slow subspaces are much smaller than that of the active subspace.

INTRODUCTION

The numerical solution of mathematical models for reaction systems in general, and reacting flows in particular, is a challenging task because of the simultaneous contribution of a wide range of time scales to the systems' dynamics. However, it is typical that the dynamics can develop very-slow and very-fast time scales separated by a range of active time scales.

An opportunity to reduce the complexity of the problem arises when the gaps in the fast/active and slow/active time scales become large. In [1], we provided an asymptotic analysis and proposed a numerical technique consisting of an algorithmic framework, named the G-Scheme, to achieve multi-scale adaptive model reduction along-with the integration of ordinary differential equations (ODEs) using objective criteria. In the G-Scheme, it is assumed that the dynamics is (locally) decomposed into active, slow, fast, and when applicable, invariant subspaces. The method is directly applicable to initial-value ODEs and (by using the method of lines) to partial differential equations (PDEs).

For irreversible (non-equilibrium) multi-scale processes, such as a detailed kinetic model (DKM), one question not addressed in [1] is how does the entropy production relate to the decomposition into fast, active, slow, and invariant subspaces. A quick qualitative answer could be obtained by establishing a correspondence among fast, active, slow, and invariant subspaces with near-equilibrium, non-equilibrium, near-frozen, and isentropic processes. Indeed, near-equilibrium and near-frozen processes are expected to be nearly isentropic (and quasi-linear), the algebraic invariants (linear and nonlinear) correspond to isentropic processes, and non-equilibrium processes are expected to be non-isentropic (and nonlinear). As a consequence, the entropic contributions of the fast and slow subspaces are expected to be small with respect to that of the active subspace. In this paper, we will analyze this aspect of the G-Scheme with the help of illustrative examples in the context of auto-ignition in a spatially homogeneous batch reactor.

Einstein's treatment [2] of the propagation of small-disturbances in a monochromatic reacting gas showed that the limiting values of frozen and equilibrium sound speeds arise as the limits for the high and low frequencies of the acoustic velocity of the linearized (about the state of thermodynamic equilibrium) wave equation with a single relaxation process.

To this regard, our discussion can be considered as an attempt at generalizing this classic finding to the case of an unlimited number of nonlinear relaxation processes, where the concepts of high and low frequencies in oscillatory phenomena are replaced by those of fast and slow subspaces of dissipative/explosive phenomena.

Theory

We would like to verify empirically the contributions of the slow, active, and fast subspaces to the overall rate of entropy production in a system featuring chemical non-equilibrium. To this end, we resort to the standard model of a constant volume, adiabatic, batch reactor, where the mixture's temperature is initially set above the auto-ignition temperature.

Batch Reactor

The set of ODEs describing the time evolution of the state of the system is:

$$\begin{aligned} \frac{\mathrm{dT}}{\mathrm{dt}} &= -\frac{1}{\rho C_p}\sum_{j=1}^{N} h_j(T) W_j \dot{\omega}_j(T,Y_j), \\ \frac{dY_j}{\mathrm{dt}} &= \frac{W_j\,\dot{\omega}_j(T,Y_j)}{\rho}, \quad j=1,\ldots,N \end{aligned} \tag{1}$$

where T and Y_j are the temperature and composition (expressed in terms of mass fractions) of the mixture, t is time, ρ is the constant mixture density, C_p is the mixture constant pressure specific heat, N is the number of species, h_j is the species enthalpy, W_j is the species molecular weight, and $\dot{\omega}_j$ is the molar rate of formation/destruction of the j-th species. The set of ODEs is closed by the thermal equation of state for a mixture of ideal

*Corresponding author: mauro.valorani@uniroma1.it

gases

$$p = \rho R(Y_j)\, T, \tag{2}$$

where p is the pressure, R is the mixture's gas constant, and the caloric equation of state

$$C_p(T, Y_j) = \sum_{j=1}^{N} C_{p,j}(T) Y_j, \tag{3}$$

where $C_{p,j}$ is the constant pressure specific heat of the j-th species.

The customary relations between mass fractions Y_j, molar fractions X_j, and molar concentrations c_j read:

$$c_j = \rho \frac{X_j}{\overline{W}} = \rho \frac{Y_j}{W_j} Y_j, \tag{4}$$

where $\overline{W}$ is the mean molecular weight of the mixture. The molar rate of formation/destruction of the j-th species reads:

$$\dot{\omega}_j(T, Y_j) = \sum_{k=1}^{K} \Delta\nu_{j,k}\, r^k(T, Y_j) \tag{5}$$

where $\boldsymbol{\nu}'_k = \nu'_{j,k}$ and $\boldsymbol{\nu}''_k = \nu''_{j,k}$ are the forward and reverse stoichiometric coefficients of the j-th species in the k-th reaction out of K total reactions, and $\Delta\boldsymbol{\nu}_k = \Delta\nu_{j,k} = \boldsymbol{\nu}''_k - \boldsymbol{\nu}'_k$ is the net stoichiometric coefficient. The net rate of the k-th reaction reads:

$$r^k(T, Y_j) = r_f^k - r_b^k = K_f^k \prod_{j=1}^{N} c_j^{\boldsymbol{\nu}'_k} - K_b^k \prod_{j=1}^{N} c_j^{\boldsymbol{\nu}''_k}, \tag{6}$$

where r_f^k and r_b^k are the forward and backward reaction rates, and K_f^k and K_b^k are the forward and backward reaction constants, which depend exponentially on temperature according to the standard Arrhenius form.

The definition of entropy of a mixture of N ideal gases used in this paper is:

$$s(T, X_j) = \sum_{j=1}^{N} \Delta s^0_{f,j}(T) X_j - R \log\left(\frac{p}{p_{\text{ref}}}\right) - R \sum_{j=1}^{N} X_j \log(X_j). \tag{7}$$

Entropy production

If the system is spatially homogeneous, the following ODE describes the time evolution of entropy (per unit mass):

$$\frac{ds}{dt} = -\frac{1}{\rho T} \sum_{j=1}^{N} \mu_j(T, Y_j)\, W_j\, \dot{\omega}_j(T, Y_j) \tag{8}$$

where $\mu_j = h_j - T s_j$ is the chemical potential (per mole unit) of the j-th species.

The net rate of the k-th reaction is usually re-written by taking advantage of the relation between the equilibrium coefficient, and the forward and backward reaction coefficients

$$K_c^k = \frac{K_f^k}{K_b^k} \tag{9}$$

to obtain

$$r^k = K_f^k \left(\prod_{j=1}^{N} c_j^{\boldsymbol{\nu}'_k} - \frac{1}{K_c^k} \prod_{j=1}^{N} c_j^{\boldsymbol{\nu}''_k} \right). \tag{10}$$

Finally, introducing the affinity (per unit mass) of the k-th reaction,

$$A_k = -\sum_{j=1}^{N} \mu_j W_j \Delta\nu_{j,k}, \tag{11}$$

allows us to cast the time evolution of entropy in the final form:

$$\frac{ds}{dt} = \frac{1}{\rho T} \sum_{k=1}^{K} A_k K_f^k \left(\prod_{j=1}^{N} c_j^{\boldsymbol{\nu}'_k} - \frac{1}{K_c^k} \prod_{j=1}^{N} c_j^{\boldsymbol{\nu}''_k} \right). \tag{12}$$

Canonical form

The set of ODEs for the batch reactor is simply a dynamical system defined by

$$\begin{gathered} \frac{d\mathbf{x}}{dt} = \mathbf{f}(\mathbf{x}), \qquad \mathbf{x}(0) = \mathbf{x}_0, \qquad \text{with} \\ \mathbf{x} \in \mathbb{R}^{N+2},\ t \in (0, T) \subset \mathbb{R},\ \text{and}\ \mathbf{f} : E \subset \mathbb{R}^{N+2} \to \mathbb{R}^{N+2}. \end{gathered} \tag{13}$$

where the state of the system is defined as $\mathbf{x} = \{Y_j, T, s\}$ and the vector field is defined by

$$\begin{aligned} \mathbf{f}(Y_j, T, s) = \Bigg\{ & \frac{W_j\, \dot{\omega}_j(T, Y_j)}{\rho},\ -\frac{1}{\rho C_p} \sum_{j=1}^{N} h_j W_j\, \dot{\omega}_j(T, Y_j), \\ & -\frac{1}{\rho T} \sum_{j=1}^{N} \mu_j(T, Y_j) W_j\, \dot{\omega}_j(T, Y_j) \Bigg\}. \end{aligned} \tag{14}$$

Note that for a constant volume system, the entropy equation is slaved to the other ODEs.

Basic Concepts for the G-Scheme

We have assumed that the dynamics is decomposed into active, slow, fast, and when applicable, invariant subspaces. The G-Scheme introduces a local curvilinear frame of reference, defined by a set of orthonormal basis vectors with corresponding coordinates, attached to this decomposition. The evolution of the curvilinear coordinates associated with the active subspace, $\Delta\xi^a$, is described by non-stiff ODEs, whereas those associated with the slow, $\Delta\xi^h$, and fast, $\Delta\xi^t$, subspaces are accounted for

by applying asymptotic approximations of the original problem to provide $\Delta\xi^h_{FF}$, and $\Delta\xi^t_{SIM}$, respectively. Adjusting the active ODEs dynamically during the time integration is the most significant feature of the G-Scheme, since the numerical integration is accomplished by solving a number of ODEs, typically much smaller than the dimension of the original problem, with corresponding savings in computational work.

The Adaptive Reduced Model

The G-Scheme involves two main stages:

1. Evolution of the active modes described by $N_{\mathbb{A}}$ non-stiff ODEs;
2. Corrections associated with the slow/fast dynamics.

The active ODEs evolve in subspace $\mathbb{A}$ which is freed from fast scales, i.e., they are non-stiff. They can be solved by resorting to any explicit scheme of integration (e.g., explicit Runge-Kutta). When compared to a standard BDF implicit scheme for stiff problems, the G - Scheme requires the solution of $N_{\mathbb{A}}$ explicit ODEs instead of $N+2$ implicit ODEs. However, the scheme requires the identification of the tangent space decomposition.

Adjusting the active ODEs dynamically is the most significant feature of the G-Scheme, because the numerical integration of a state vector $\mathbf{x} \in N+2$ is obtained by solving a number ($\ll N$) non-stiff ODEs with the corresponding saving in CPU work.

Tangent Space Decomposition

Ideal decomposition of the tangent space $\mathcal{T}_{\mathbf{x}}$ at any point $\mathbf{x} \in \mathbb{C} \subset \mathbb{R}^{N+2}$ involves the identification of $N+2$ invariant subspaces, a difficult task. The G-Scheme decomposes the tangent space in four subspaces having time scales of comparable magnitude, $\mathcal{T}_x = \mathbb{E} \oplus \mathbb{H} \oplus \mathbb{A} \oplus \mathbb{T}$, where $\mathbb{E}$ is the linear subspace spanned by directions associated with invariants, if any exists (conservation laws). All scales slower than the active ones are confined to the slow subspace $\mathbb{H}$(ead) (dormant/near-frozen processes). The active subspace $\mathbb{A}$ contains all the current intermediate dynamic time scales (active/non-equilibrium). All scales faster than the active ones are confined in the fast subspace $\mathbb{T}$(ail) (exhausted/near-equilibrium). Thus, the basic concept in the G-Scheme is to 'distill' the Heart, and 'cut' the Head and Tail in a generic multi-scale dynamical system.[1]

Basis Vectors and Time Scales

The most important decision to be taken in the implementation of the G-Scheme framework is the choice of a curvilinear frame of reference, i.e., a basis matrix yielding a maximal degree of slow/fast decoupling. In fact, the basis vectors used to define the matrix might be found, in principle, by different means, if they can provide the ideal block-diagonalization of the eigenvalue matrix in a cost efficient way. The Computational Singular Perturbation [3] method offers a computational algorithm to achieve this goal. The CSP refinements converge to the right/left eigenvectors of $J(\mathbf{x}(t_n))$ if nonlinearities are neglected. In this case, we can rank the basis vectors according to the magnitude of the corresponding eigenvalues, to obtain

$$0 = \lambda_1 = \cdots = \lambda_E < |\lambda_{E+1}| \leq \cdots \leq |\lambda_{H-1}| \ll |\lambda_H| \leq \cdots \leq |\lambda_T| \ll |\lambda_{T+1}| \leq \cdots \leq |\lambda_{N+2}|, \tag{15}$$

where

$$\begin{aligned} 0 = \lambda_1 = \cdots = \lambda_E &\quad \text{identify the scales in } \mathbb{E}, \\ |\lambda_{E+1}| \leq \cdots \leq |\lambda_{H-1}| &\quad \text{identify the scales in } \mathbb{H}, \\ |\lambda_H| \leq \cdots \leq |\lambda_T| &\quad \text{identify the scales in } \mathbb{A}, \\ |\lambda_{T+1}| \leq \cdots \leq |\lambda_{N+2}| &\quad \text{identify the scales in } \mathbb{T}. \end{aligned} \tag{16}$$

As estimate of the time scale associated to an eigendirection, we take the inverse of the magnitude of the corresponding eigenvalue.

Asymptotics of Fast and Slow Time Scales

The G-Scheme exploits the two archetypes for reduction, slow-invariant-manifold (SIM) and fast-fibers (FF), to define the adaptive reduction: SIM and FF concepts are invoked to define the T(ail) and H(ead) subspaces, respectively. The concepts of SIM and FF are invoked on a local basis. Differently from other approaches, for the G-Scheme to be applicable it is not required that a global SIM exist, nor that the SIM dimension be constant or prescribed in advance. Similar comments apply for the exploitation of the FF. The contributions of fast and slow scales are accounted for with SIM and FF algebraic corrections obtained through asymptotic analysis.

The G-Scheme Step-by-Step

The following section is illustrated in full detail in [1], and is reported here for the reader convenience. For time interval t_0,and for the state vector $x(t_0)$, initialize the integration as:

1. Compute:
   $T(x(t_0)) = N, J(x(t_0))$, $\lambda_i(x(t_0))$, $A(x(t_0))$, $B(x(t_0))$
   where J is the Jacobian matrix of the vector field of Eq. (13), λ_i is the eigenvalue of the i-th eigenmode of J, and the matrix A/B collect all the right (row)/left(column) eigenvectors of J; T is a scalar value denoting the fastest of the active modes..
   For each time interval t_n (τ = 0), and for the state vector $x(t_n)$, with n = 0, 1, 2, . . , proceed as follows:
2. Define Time Step as : $\Delta t = \gamma / \left|\lambda_{T(x(t_n))}\right|$ $\gamma \approx O(1)$;
3. Update Time : $t_{n+1} = t_n + \Delta t$;
4. Identify the Head Subspace dimension, $H(x(t_n))$ on the basis of a user specified accuracy vector defined as $\varepsilon_{acc} = rtol|y_j| + atol$;
5. Solve the set of non-stiff Active ODE' s:

$$\frac{d\Delta\xi^a(\tau)}{d\tau} = B^a(t_n) f[x(t_n) + A_a(t_n)\Delta\xi^a(\tau)] \tag{17}$$

   with $\Delta\xi^a(0) \equiv 0^a \qquad a = H, T$.
6. Update state vector: $x^a(t_{n+1}) = x(t_n) + A_a(t_n)\Delta\xi^a(\Delta t)$
7. Apply Head Correction:
   $x^h(t_{n+1}) = x^a(t_{n+1}) + A_h(t_n)\Delta\xi^h_{FF}(\Delta t)$

[1] G stands for Grappa, an Italian liquor produced by distillation.

$$\Delta\xi^{s}_{\mathrm{FF}}(\Delta t) \approx \Delta t\left[I+\frac{1}{2}\Lambda^{s}_{s}\left(x\left(t_n\right),0\right)\Delta t\right]B^{s}(0)f\left(x\left(t_n\right)\right) \approx \Delta t B^{s}(0)f\left(x\left(t_n\right)\right) \quad (18)$$

8. Apply First Tail Correction:
   $x^{t}\left(t_{n+1}\right)=x^{h}\left(t_{n+1}\right)+A_{t}\left(t_n\right)\Delta\xi^{t}_{\mathrm{SIM}(t_n)}(\Delta t)$

$$\Delta\xi^{r}_{\mathrm{SIM}}\left(x^{*}\right) = -\left(B\left(x^{*}\right)J(x^{*})A_{r}(x^{*})\right)^{-1}B\left(x^{*}\right)f\left(x^{*}\right) \quad (19)$$

9. Update
   $\mathrm{J}(x^{t}\left(t_{n+1}\right))$, $\lambda_{i}\left(x^{t}\left(t_{n+1}\right)\right)$, and $\mathrm{A}(x^{t}\left(t_{n+1}\right))$, $\mathrm{B}(x^{t}\left(t_{n+1}\right))$
10. Apply Second Tail Correction
    $x\left(t_{n+1}\right)=x^{t}\left(t_{n+1}\right)+A_{t}\left(t_{n+1}\right)\Delta\xi^{t}_{\mathrm{SIM}(t_{n+1})}(\Delta t)$

$$\Delta\xi^{r}_{\mathrm{SIM}}\left(x^{*}\right) = -\left(B\left(x^{*}\right)J(x^{*})A_{r}(x^{*})\right)^{-1}B\left(x^{*}\right)f\left(x^{*}\right) \quad (20)$$

11. Identify the Tail Subspace dimension, $T\left(x\left(t_{n+1}\right)\right)$ on the basis of the user specified accuracy vector ε_{acc};
12. Update counter n=n+1
13. If$[\ t_{n+1}<t_{f}]$ go to Step (1)

The numerical solution generated by the G-Scheme approximates the trajectory of the original system by patching together trajectories obtained with reduced order models, each lying on the corresponding SIM (Fig.1). All the trajectories describing

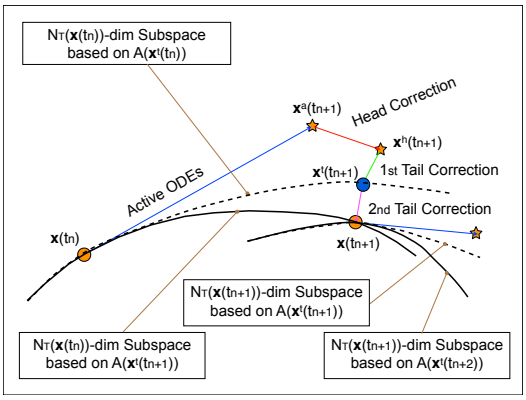

Figure 1. Sketch of the G-Scheme algorithm (reprinted from [1]).

the transients between different SIMs in the original system (together with the associated fast scales) are not represented by the G-Scheme-generated solution, since their overall contribution to the system dynamics are accounted for by projection operations.

Entropy Production and the G-Scheme

We are now ready to analyze qualitatively the contributions of the slow and fast subspaces to the overall rate of entropy production in a system featuring chemical non-equilibrium. To simplify the illustration of the concept, let us consider (i) the contribution of a single, say the k-th, reaction to the rate of entropy production:

$$\frac{\mathrm{ds}}{\mathrm{dt}}=\frac{A_k}{\rho \mathrm{T}}K^{k}_{f}\left(\prod_{j=1}^{N}c_j^{\nu'_k}-\frac{1}{K^{k}_{c}}\prod_{j=1}^{N}c_j^{\nu''_k}\right), \quad (21)$$

and (ii) that the basis vectors used to define the matrix A returns a simple identity matrix.

Entropy Production from Head

The contribution to the rate of entropy production of the k-th reaction evaluated using Eq.(18) reads:

$$\Delta\xi^{h}_{\mathrm{FF}}\left(\Delta t_r\right) \approx \Delta t f\left(x\left(t_n\right)\right) \approx -\left(K^{k}_{f}\Delta t\right)\frac{A_k}{\rho \mathrm{T}}\left(\prod_{j=1}^{N}c_j^{\nu'_k}-\frac{1}{K^{k}_{c}}\prod_{j=1}^{N}c_j^{\nu''_k}\right) \quad (22)$$

The product $K^{k}_{f}\Delta t$ is small when the k-th reaction is slow, i.e., when $K^{k}_{f}\ll 1$, that is $\tau^{k}_{\mathrm{slow}}=1/K^{k}_{f}\gg 1$. Note that the currently active scale is given by $\tau_T\sim 1/|\lambda_T|$, and we take $\Delta t\sim\tau_T$. Subsequently, we have that $K^{k}_{f}\Delta t\sim O(\tau_T/\tau_{\mathrm{slow}})\ll 1 \implies \Delta\xi^{h}_{\mathrm{FF}}\left(\Delta t_r\right)\sim O(\tau_T/\tau_{\mathrm{slow}})\ll 1$, that is the contribution to the rate of entropy production of the k-th reaction on the slow subspace is of the order of the ratio between the currently active scale and the fastest of the slow scales, and thus:

$$s^{h}\left(t_{n+1}\right)=s^{a}\left(t_{n+1}\right)+\Delta\xi^{h}_{\mathrm{FF}}(\Delta t)\sim s^{a}\left(t_{n+1}\right)+O(\tau_T/\tau_{\mathrm{slow}}).$$

Entropy Production from Tail

Suppose that the k-th reaction is in near-equilibrium, so that the law of mass action is approximately valid to yield:

$$\left(\prod_{j=1}^{N}c_j^{\nu'_k}-\frac{1}{K^{k}_{c}}\prod_{j=1}^{N}c_j^{\nu''_k}\right)\ll 1. \quad (23)$$

Next, consider the contribution to the rate of entropy production of the k-th reaction evaluated using Eqs.(19-20) reads.

$$\begin{aligned}\Delta\xi^{r}_{\mathrm{SIM}}\left(x^{*}\right) &= -\left(B\left(x^{*}\right)J(x^{*})A_{r}(x^{*})\right)^{-1}f\left(x^{*}\right)\\ &\sim -\frac{1}{|\lambda(x^{*})|}f\left(x^{*}\right)\\ &\sim -\frac{K^{k}_{f}}{|\lambda(x^{*})|}\frac{A_k}{\rho \mathrm{T}}\left(\prod_{j=1}^{N}c_j^{(\nu')_k}-\frac{1}{K^{k}_{c}}\prod_{j=1}^{N}c_j^{(\nu'')_k}\right)\end{aligned} \quad (24)$$

As a consequence, the contribution of the tail to the rate of entropy production becomes

$$\Delta\xi^{t}_{\mathrm{SIM}}\left(x^{*}\right)=-\left(K^{k}_{f}\Delta t\right)\frac{A_k}{\rho \mathrm{T}}\left(\prod_{j=1}^{N}c_j^{\nu'_k}-\frac{1}{K^{k}_{c}}\prod_{j=1}^{N}c_j^{\nu''_k}\right), \quad (25)$$

that is the contribution to the rate of entropy production of the k-th reaction on the fast subspace is negligible because of Eq. (23) even if $K_f^k \gg 1$, as is the case for fast reactions, and therefore:

$$\begin{aligned} s^t(t_{n+1}) &= s^h(t_{n+1}) + \Delta\xi^t_{\mathrm{SIM}(t_n)} \sim s^h(t_{n+1}) \\ s(t_{n+1}) &= s^t(t_{n+1}) + \Delta\xi^t_{\mathrm{SIM}(t_{n+1})} \sim s^t(t_{n+1}). \end{aligned} \tag{26}$$

RESULTS

The specific test case considered refers to a methane/air system, using GRI 3.0 kinetics (53 species). The batch reactor model is adiabatic and at constant volume. The initial conditions for the test case are defined by prescribing the initial temperature $T_0 = 1000\ K$ and pressure $p_0 = 1\ atm$ of a stoichiometric mixture of reactants. The constant density in Eq. (1) is set on the basis of the thermal equation of state.

Figure 2 shows the evolution of temperature (solid, black line) as a function of the number of iteration steps (to avoid the compression of the plot about the reaction time). On the same figure, we plot the evolution of the dimension A of the active subspace (green solid line) obtained by subtracting H (blue line) from T (red line), where H and T are the mode numbers corresponding to $|\lambda_H|$ and $|\lambda_T|$, respectively. The dimension of the active subspace also corresponds to the number of non-stiff ODEs solved by the G-Scheme. The modes comprised between 5 and H-1 span the slow subspace, those between H and T the active subspace, and those between T+1 and N+2 the fast subspace.

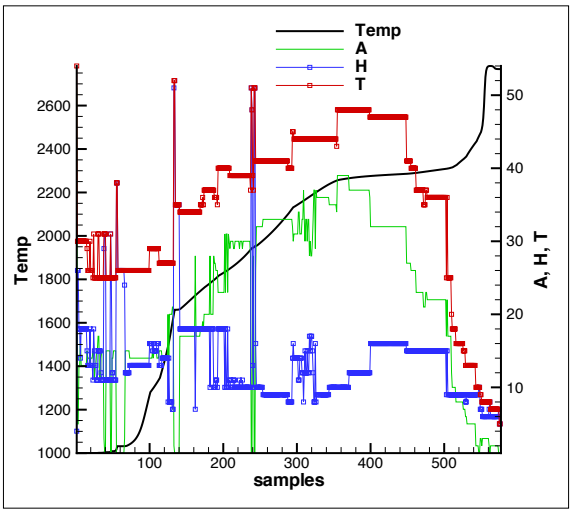

Figure 2. Time evolution of the dimension of the active (green), slow (blue), and fast (red) subspaces; temperature (solid black line); $rtol = 10^{-3}$.

Figure 3 shows the time evolution of the reciprocal of the modulus of the (complex) eigenvalues of the 55 modes as a function of the number of iteration steps. On the same figure, we plot the evolution of the characteristic scales of the G-Scheme, namely, the reciprocal of $|\lambda_{H-1}|$ (green), $|\lambda_H|$ (red), $|\lambda_T|$ (cyan), $|\lambda_{T+1}|$ (blue), and $|\lambda_{N+2}|$ (black). The blue solid line reports the entropy evolution. The slow/active scale gap is is visually comprised between the green and red lines, while the active/fast gap is between the cyan and blue lines. The black line marks the fastest time scale at all times. The spectral width of the fast subspace is between the black and blue lines. The width of the active subspace is between the cyan and red lines. The width of the slow subspace is above the red line. The invariant subspace is associated with the randomly scattered markers visible at very large time scales.

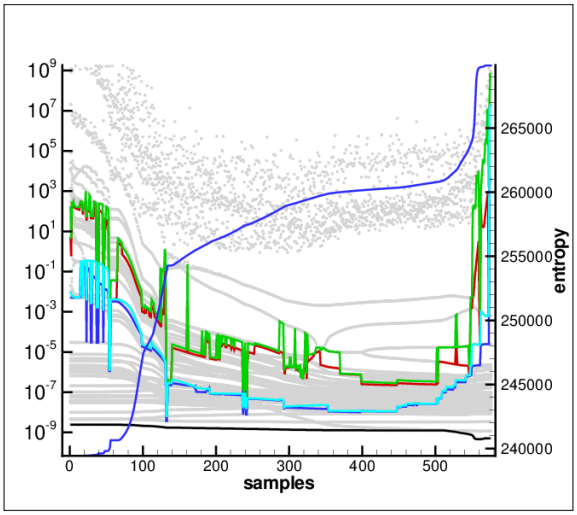

Figure 3. Reciprocal of the modulus of the (complex) eigenvalues (light grey markers); reciprocal of $|\lambda_{H-1}|$ (green), $|\lambda_H|$ (red), $|\lambda_T|$ (cyan), $|\lambda_{T+1}|$ (blue), and $|\lambda_{N+2}|$ (black); the red solid line reports the entropy evolution; $rtol = 10^{-3}$.

The quantitative assessment of the relative contribution to the rate of entropy production from the slow, active, and fast subspaces is carried out by considering that the entropy of the mixture is a state function of temperature and composition. Therefore, during the numerical integration of the batch reactor model, we evaluated the entropy of the mixture before and after each of the changes of the system state due to the slow (Δs_h), active (Δs_a), and fast (Δs_t) subspaces. With these definitions, we introduced the following:

$$\begin{aligned} s_a(t_n) &= s_a(t_{n-1}) + \Delta s_a(t_n) \\ s_h(t_n) &= s_h(t_{n-1}) + \Delta s_h(t_n) \\ s_t(t_n) &= s_t(t_{n-1}) + \Delta s_t(t_n) \\ s(t_n) &= s_a(t_n) + s_h(t_n) + s_t(t_n) \end{aligned} \tag{27}$$

where $s_\alpha(t_0) = s(T_0, p_0, Y_{j,0}), \alpha = a,h,t$. Figure 4 shows the time evolution of the contribution to the entropy of the mixture from the slow, active, and fast subspaces as obtained using three different accuracy levels ($rtol = 10^{-3}, 10^{-4}, 10^{-5}$), while Fig. 5 shows the entropy contribution of each subspace scaled with respect to the overall contribution ($s_\alpha(t_n)/s(t_n)$ with $\alpha = a,h,t$). It is apparent that the active subspace contribution is always very close to 100%, while the slow contribution is generally larger than the fast contribution.

The sensitivity to the accuracy level of the contribution to the entropy of the mixture can be appreciated with the help of Fig 6, which indicates that the magnitude of the overall entropy contribution, that is, evaluated at large times, of the fast subspace

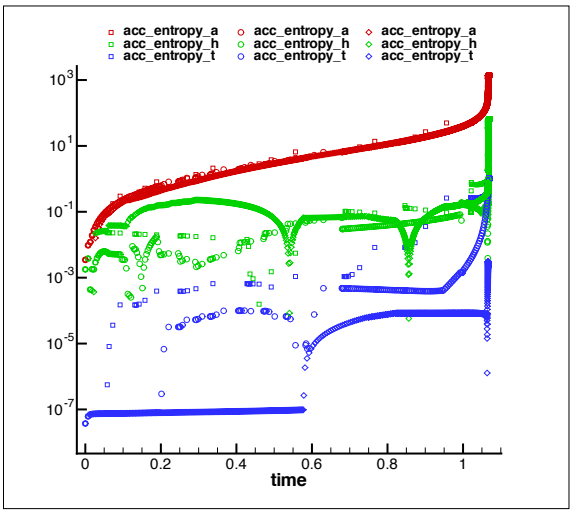

Figure 4. Contribution to the entropy of the mixture from the slow ($s_h(t_n)$, green), active ($s_a(t_n)$, red), and fast ($s_t(t_n)$, blue) subspaces, as obtained using three different accuracy levels ($rtol = 10^{-3}$ (square markers), 10^{-4} (circles), 10^{-5} (diamonds)).

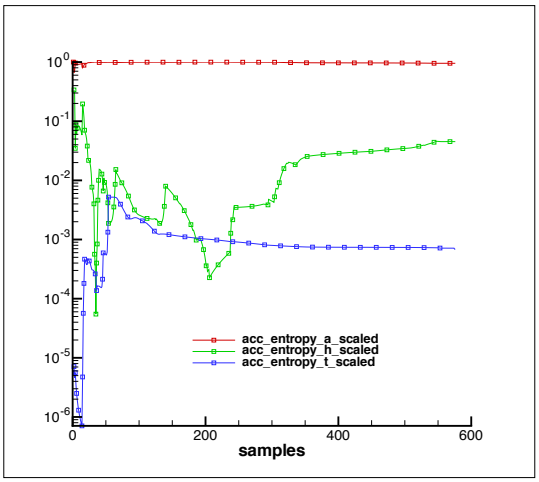

Figure 5. Contribution to the entropy of the mixture from the slow ($s_h(t_n)/s(t_n)$, green), active ($s_a(t_n)/s(t_n)$, red), and fast ($s_t(t_n)/s(t_n)$, blue) subspaces scaled with respect to the overall contribution ($rtol = 10^{-3}$).

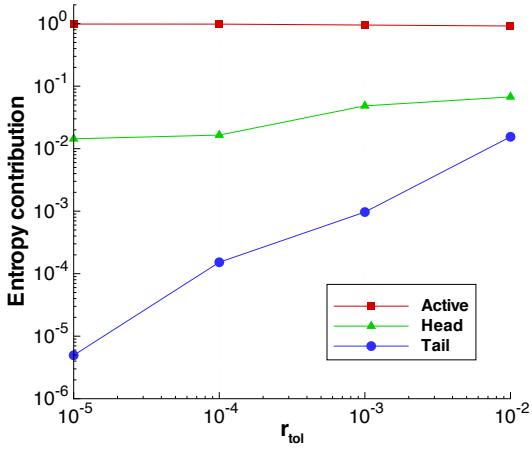

Figure 6. Overall entropy production per each subspace; slow ($s_h(t_\infty)$, green), active ($s_a(t_\infty)$, red), and fast ($s_t(t_\infty)$, blue) subspaces.

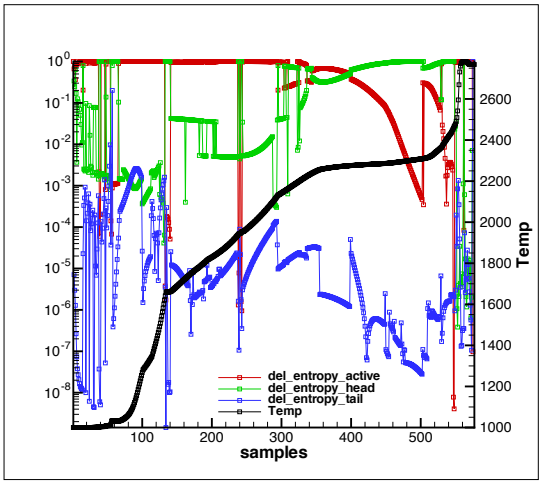

Figure 7. Contribution to the rate of change of entropy of the mixture from the slow ($\Delta s_h(t_n)/\Delta s(t_n)$, green), active ($\Delta s_a(t_n)/\Delta s(t_n)$, red), and fast ($\Delta s_t(t_n)/\Delta s(t_n)$, blue) subspaces ($rtol = 10^{-3}$).

is of the same order of the accuracy level specified by the user. Instead the overall entropy contribution of the slow subspace is always smaller than the active contribution, but it does not seem to depend much on the accuracy level specified by the user.

Figure 7 shows that the relative contribution to the rate of entropy production ($\Delta s_\alpha(t_n)/\Delta s(t_n)$) of the slow and fast subspaces are approximately 10^{-3} and 10^{-4}, respectively, whereas that of the active subspace is always of order one. This indicates that the contribution to the rate of entropy production of the fast subspace is always negligible with respect to that of the active subspace, whereas that of the slow subspace can occasionally becomes comparable to that of the active subspace within the reaction period of the auto-ignition process.

CONCLUSIONS

Reaction systems are characterized by the simultaneous presence of a wide range of time scales. When the dynamics of reactive systems develop very-slow and very-fast time scales separated by a range of active time scales, with large gaps in the fast/active and slow/active time scales, then it is possible to achieve multi-scale adaptive model reduction along-with the integration of the ODEs using the G-Scheme framework. The G-Scheme assumes that the dynamics is decomposed into active, slow, fast, and invariant subspaces. To calculate the contribution to entropy production related to the four subspaces, we resorted to a standard model of a constant volume, adiabatic, batch reactor, where the mixture temperature of the reactants is initially set above auto-ignition temperature. The specific test case considered refers to a methane/air system, using GRI 3.0 kinetics. The numerical experiments indicate that the contributions of the fast and slow subspaces are typically much smaller (of the order of the user defined accuracy of the numerical integration) both locally and globally than the contribution of the active subspace. A preliminary analysis of the relevant theory is offered to indicate why this conclusion might be of general validity.

ACKNOWLEDGMENT

MV acknowledges the support of the Italian Ministry of University and Research (MIUR).

References

[1] M Valorani and S Paolucci. "The G-Scheme: A framework for multi-scale adaptive model reduction". In: *Journal of Computational Physics* 228.13 (2009), pp. 4665–4701.

[2] A. Einstein. "Schallgeschwindigheit in teilweise dissoziierten Gasen". In: *Sitzungsberichte d. preussischen Adak. d. Wiss. Wien* 18.1 (1920), p. 380.

[3] S. H. Lam and D. a. Goussis. "The CSP method for simplifying kinetics". In: *International Journal of Chemical Kinetics* 26.4 (Apr. 1994), pp. 461–486. ISSN: 0538-8066. DOI: 10.1002/kin.550260408. URL: http://doi.wiley.com/10.1002/kin.550260408.